Journal of Machine Engineering, 2019, Vol. 19, No. 2, 5–17
ISSN 1895-7595 (Print) ISSN 2391-8071 (Online)

Received: *20 December 2018* / Accepted: *06 May 2019* / Published online: *29 June 2019*

linear motor, control, feed drive

Steffen IHLENFELDT[1,2]
Jens MÜLLER[1]
Marcel MERX[1*]
Christoph PEUKERT[1]

DESIGN APPROACH FOR HIGH-DYNAMIC PLANAR MOTION SYSTEMS BASED ON THE PRINCIPLE OF KINEMATICALLY COUPLED FORCE COMPENSATION

Machine tools' feed dynamics are usually limited in order to reduce excitation of machine structure oscillations. Consequently, the potential increase in productivity provided by direct drives, e.g. linear motors, cannot be exploited. The novel approach of the Kinematically Coupled Force Compensation (KCFC) applies a redundant axis configuration combined with the principle of force compensation and thus achieves an increase in feed dynamics while drive reaction forces cancel out each other in the machine base. In this paper, the principle of KCFC is introduced briefly. Subsequently, the basics for the realisation of a highly dynamic KCFC motion system with planar motion are derived and discussed. In order to achieve highest acceleration (> 100 m/s²) and jerk (> 100000 m/s³), a mechatronic system with specially designed components for the mechanical, electrical and control system is required. Thus, the design approach presented in this paper applies lightweight slides, a decoupled guide frame and voice coil motors operated at high frequencies for the pulse width modulation and control loops.

1. INTRODUCTION

This paper presents a novel design approach for highly dynamic planar motion systems, enabling increased feed dynamics under preservation of motion quality. The applied principle of Kinematically Coupled Force Compensation (KCFC) is presented, assigned into the state of the art and the basics for the realisation of a 2D-KCFC motion system are derived.

The generation of freely programmable, precise and at the same time dynamic motions, provides the basis for a large number of machining processes and enables their effective use. The further development of the process-executing motion systems is motivated by the trend towards individualisation, which is synonymous with smaller batch sizes and simultaneously high or even increasing productivity requirements. Considering the motion systems, this leads

[1] TU Dresden, Faculty of Mechanical Science and Engineering, Institute of Mechatronic Engineering, Chair of Machine Tools Development and Adaptive Controls, Dresden, Germany
[2] Fraunhofer Institute for Machine Tools and Forming Technology IWU, Dresden, Germany
[*] E-mail: marcel.merx@tu-dresden.de
https://doi.org/10.5604/01.3001.0013.2175

to increasingly powerful drives (e.g. use of linear direct drives, also as parallel drives [1]), which are installed in machine structures with highest possible damping and controlled by means of optimised control algorithms [2, 3]. With the drive technology available today, especially with linear direct drives, it is possible to achieve accelerations up to 50 m/s² [4]. This means that the current generation of machines makes the best possible use of the given acceleration capacity of the drives. In contrast, the possible change in acceleration – the jerk – is typically limited by the machine control in order to reduce the vibrational excitation of the machine structure to a tolerable level. This is necessary because a high jerk value corresponds to a high force rise rate, which in the frequency domain causes a broadband excitation of the machine's base frame. As shown on the analogy model of the single mass oscillator in Fig. 1a, the excited oscillation is transmitted via the kinematic chain to the tool centre point (TCP) and imprinted there as contour or surface deviation in the workpiece. In practice, values in the range of some 100 m/s³ for machines with electromechanical drives via ball screw and values in the range of 1000 m/s³ for machines with linear direct drives [5] are set for the jerk limitation. Depending on the linear motor type and the moving mass of the slide, the technically possible jerk values are in the range of 10000 m/s³ to 100000 m/s³. A high jerk is particularly important for trajectories with frequent changes of direction. This is the case, for example, with the machining of free-form surfaces, which require smallest motion segments.

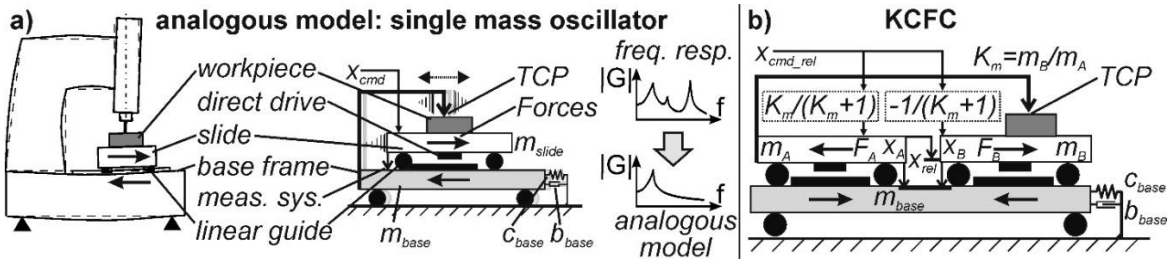

Fig. 1. a) Analogy model for the representation of the dominant eigenmode of a machine frame according to [6]; b) Schematic diagram of the Kinematically Coupled Force Compensation (KCFC) according to [7, 8]

In order to exploit the dynamic potential of direct drives, various approaches for the modification of machine structures and drive systems have been developed and investigated. Some of these methods, such as force decoupling (also known as jerk decoupling), force compensation and redundant axis configurations, are compared in [6]. Force compensation uses a counterforce acting on the underlying machine structure synchronously to the motion of the actual feed drive by means of a compensation drive. If the compensation drive is now included in the kinematic chain to the TCP, the KCFC is obtained (Fig. 1b). In KCFC the relative motion at the TCP is distributed to both slides m_A and m_B, taking into account the mass ratio K_m, whereby the drive reaction forces F_A and F_B cancel out each other under ideal conditions. In this redundant axis configuration the motions of the slides add up at the TCP according to $x_{TCP} = x_A + x_B$ [7].

The KCFC has already been implemented in a test bed with uniaxial motion (1D-KCFC) and its functionality has been demonstrated [8]. Alternative control structures with superimposed position or superimposed position and velocity control (cf. [7] and [8]) have

also successfully been tested. The superimposed position and velocity control is particularly promising, since it enables direct control of the relative position measured between the slides near to the TCP (see x_{rel} in Fig. 1b). A further control loop ensures that a defined position is maintained relative to the frame (x_A or x_B in Fig. 1b).

As shown in [7], the KCFC can be implemented in a variety of kinematic configurations. Fig. 2a shows a linear arrangement on the example of a surface grinding process. In this case the force flow of the drive reaction forces takes place via the frame as a tension-compression force. In the configuration with planar motion in the *X*- and *Y*-direction shown in Fig. 2b, dynamic torque is generated because of the forces applied in two different Z-planes. This may cause structural excitation and should be considered. A cross guide is used as guiding system to enable planar motion. Fig. 2c shows an example of a KCFC kinematic system with a rotary-linear motion. Force transmission of the rotary motion takes place as torque and the force transmission of the linear motion as tension-compression force.

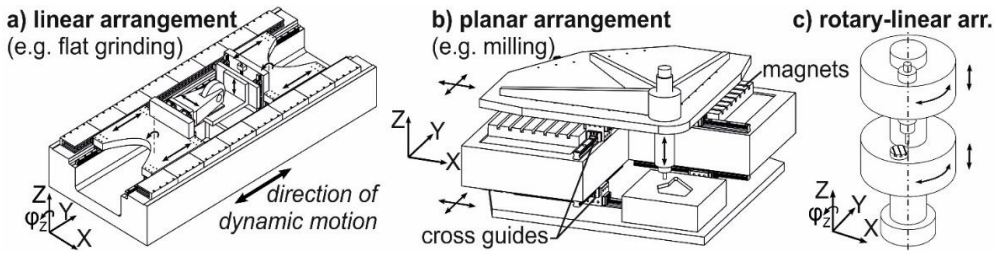

Fig. 2. Exemplary kinematics for the KCFC with direct force transmission into the frame according to [7]

In order to realise the KCFC in more than two degrees of freedom (d.o.f.), the force flow must be directed through the moving elements, e.g. the slides, which means that the advantage of direct force transmission into the frame assembly is lost. However, many motion-guided machining, handling and measurement processes require highly dynamic planar motion. The motion in normal direction (usually *Z*-axis) is subordinate in terms of productivity. Therefore, this paper focuses on the design of planar motion systems according to the KCFC principle (2D-KCFC) on the example of a test bed for the experimental investigation of the method. In the following chapter, highly dynamic planar motion systems and relevant processes are presented exemplarily.

Subsequently, in the third chapter, the requirements for the 2D-KCFC motion system are defined and possible kinematic concepts are discussed. The fourth chapter is dedicated to the design of the machine structure, while the fifth chapter deals with the design of the drive system. Finally, the sixth chapter summarises the findings obtained and gives an outlook on future simulation-based analysis of the 2D-KCFC motion system.

2. HIGHLY DYNAMIC MOTION SYSTEMS AND PROCESSES

In this Chapter, the state of the art in the field of redundant and highly dynamic motion systems is presented and typical applications and processes are described exemplarily.

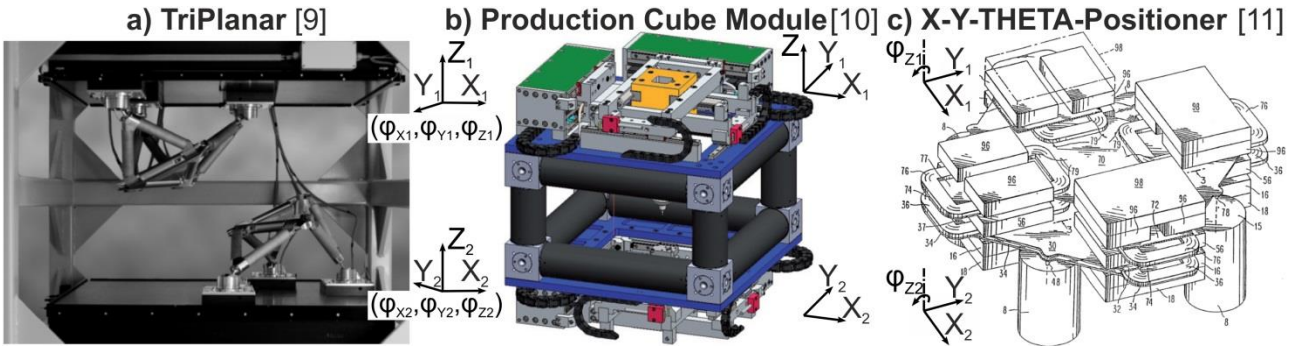

Fig. 3. Highly dynamic planar motion systems according to [9–11]

The TriPlanar is a 6 d.o.f. parallel kinematic system, which is driven at the base points of the struts by three air-bearing planar stepper motors [9]. Fig. 3a shows an arrangement of two cooperating TriPlanar kinematics, offering a large working area relative to the base area and a maximum inclination angle of each platform up to 30°. The Production Cube Module shown in Fig. 3b, developed within the Priority Program No. 1476 "Small Machine Tools for small Workpieces" of the German Research Foundation, is also a redundant kinematic system. It has been designed in order to achieve a favourable ratio of machine volume to workspace volume, considering small workpieces [10].

The compensation of the drive reaction forces has not been taken into account, especially since the drive forces are indirectly applied to the slides via motion links. In contrast, the planar motion system developed by IBM (Fig. 3c) enables the highest feed dynamics of the three systems in Fig. 3 (max. acceleration a_{max} = 1343 m/s² with a moving mass m = 42 g according to [11]). This is achieved by means of voice coil motors whose coils are embedded in the slide plate. The configuration in Fig. 3.c has a second, identical slide plate with identical motors for compensation of drive reaction forces (force compensation). However, the system does not make use of the relative motion between the slides.

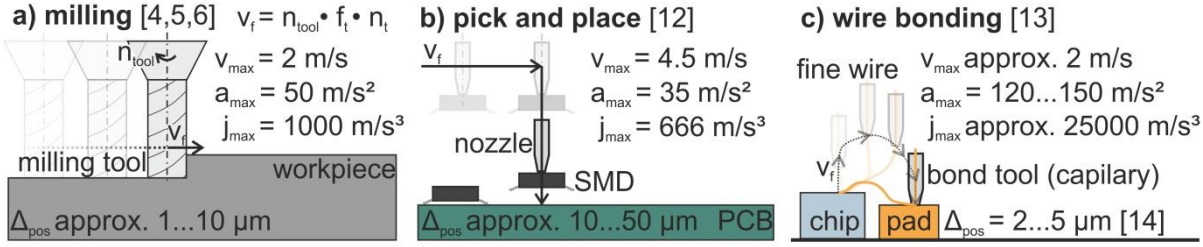

Fig. 4. Processes with highly dynamic motion according to [4–6, 12–14]

In general, there is a large number of possible applications for motion systems based on the KCFC principle. Fig. 4 shows three typical highly dynamic motion-guided processes with small workspace. The milling of workpieces (< 100 mm) with small tools (d_{tool} < 6 mm), shown in Fig. 4a, has the lowest feed rates v_f. On milling machines, the maximum feed rate v_{max} is typically only used for rapid traverse, e.g. for tool change. However, milling processes involve the greatest variety and complexity of trajectories. Similar dynamic requirements can

be found in the assembly of electronic components (pick and place of surface mounted devices – SMD – according to Fig. 4b. In contrast to milling, mostly simple point-to-point motions are carried out with maximum feed dynamics. The highest dynamic requirements can be found in the field of semiconductor processing (wire bonding in Fig. 4c). In this process, semiconductor components are electrically contacted with thin wires (e.g. gold wires) to the terminals of their housing or to a printed circuit board (PCB). In accordance with the small dimensions of the components, the requirements for the repeat accuracy of positioning Δ_{pos} are extremely high, especially considering the extraordinary feed dynamics applied.

3. REQUIREMENTS AND CONCEPTS FOR THE 2D-KCFC MOTION SYSTEM

In this Chapter, the requirements for the 2D-KCFC motion system to be developed are concretised and possible drive configurations are roughly designed and evaluated. The definition of requirements is based on highly dynamic processes according to Fig. 4. For the effective utilisation of the KCFC exclusively for motions with the highest dynamic requirements, further machining stations for subordinate processes, such as loading and unloading or calibration of the workpiece, are to be provided. The feed dynamics of the relative motion at the TCP should be at least $v_{max\_TCP} = 2$ m/s, $a_{max\_TCP} = 100$ m/s² and $j_{max\_TCP} = 100000$ m/s³ in a square working area of $x_{max} = y_{max} = 80$ mm. Process forces are assumed to be negligible. A mass ratio of $K_m \approx 1$ and thus the distribution of the relative motion to the slides in a ratio close to 1:1 is supposed. Since the experimental investigation of 2D-KCFC focuses on the generation of motion in *X*- and *Y*-direction, substitute masses of $m_{Z\text{-}axis} = 5$ kg are assumed instead of a real *Z*-axis carrying workpiece or tool respectively. Consequently, stacking of the *X*- and *Y*-axes, e.g. as a cross table, should be avoided, as this would lead to additional flexibility in the force flow. This requirement results in a favourable design of the slides as plates, comparable with the designs in Fig. 2b and Fig. 3c. The slide plates are to be designed as lightweight structures, whereby according to [15], the driving force should be applied in the centre of gravity (COG) of the moving assembly in order to reduce the excitation of tilting vibrations. A maximum mass of $m_A = m_B = 5$ kg is estimated for the slide assembly (without workpiece holder or *Z*-axis). A planar guide system, preferably based on profile rail guides, should be selected as guide system (see cross guides in Fig. 2b). Compact optical or magnetic linear scales with resolutions in the sub-µm range are to be used as measuring systems. In addition and for the superimposed position and velocity control (see [7, 8]), a planar measuring system (optical cross grid measuring device) should be applied to directly measure the relative position between the two slide plates as close as possible to the TCP. Voice coil motors are used for the drive system for the *X*- and *Y*-direction, as these allow high feed dynamics at a low axis stroke of approx. 40 mm and do not stress the slide plates with magnetic attraction forces. In order to achieve a high motor force constant k_{Mot}, the magnets are arranged in a U-shaped magnet yoke. In this yoke, four permanent magnets lie opposite to each other in the air gap (see Fig. 8). The magnets are larger than the motor coils, to ensure a homogeneous magnetic field in the entire travel range. Due to the low inductivities of the coils, high frequencies for pulse width modulation (PWM), well above the typical value of 16 kHz, should be used to keep the current ripple low.

Under the given objectives of highest possible dynamic stiffness (high eigenfrequencies) and lowest masses, three drive configurations for the 2D-KCFC were defined and the resulting design for the slide plates was derived. Fig. 5 sketches the slide plates including the motor coils and guiding system as well as the arrangement of the cross grid measuring device. For reasons of clarity, the Z-axis units and the second, lower slide plate are not depicted.

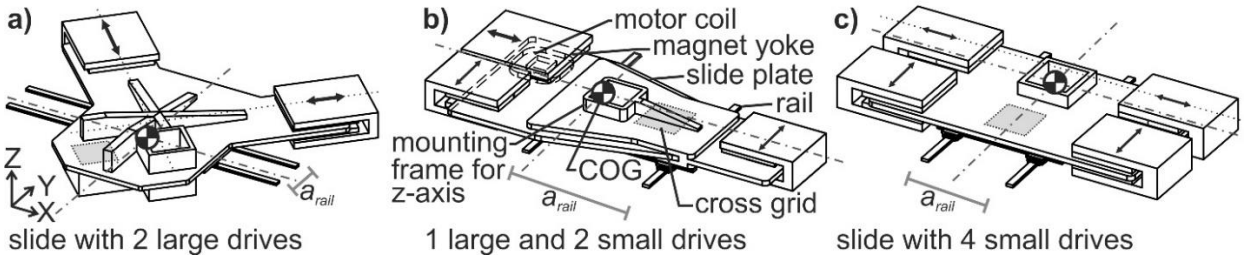

Fig. 5. Design concepts for the 2D-KCFC motion system

The design shown in Fig. 5a with two large drives is based on the concept introduced in Fig. 2b. It enables the application of the motor forces approximately in the centre of gravity (COG) of the slide plate and allows very good accessibility to the TCP. In order to achieve this, however, a small distance between the guides a_{rail} and a large overhang of the COG must be accepted. In addition, with this design it is difficult to approach further processing stations in the *X*-direction. The design shown in Fig. 5b has one large and two small drives. It offers very good accessibility to further processing stations in the *Y*-direction and enables a large distance between the guides a_{rail} due to the arrangement of the cross grid next to the *Z*-axis unit. The space requirement for the large coil also results in a wide overhang of the slide in the negative *X*-direction. The design shown in Fig. 5c overcomes the disadvantages of concepts a) and b) by a symmetrical arrangement of four small drives and the arrangement of the cross grid in front of the *Z*-axis unit. This results in a smaller distance between the guides a_{rail} and, moreover, in the lowest mass of the slide plate in comparison with the other designs. However, it must be ensured that the *Z*-axis or workpiece respectively do not collide with the measuring head or the grid plate of the cross grid measuring device. The variant according to Fig. 5c is selected for further development of the test bed. The test bed shall integrate the control cabinet and an enclosure. It should be transportable with a maximum footprint of 1200 mm × 800 mm and a weight of less than 1000 kg.

4. DESIGN AND ANALYSIS OF THE STRUCTURAL COMPONENTS

A welding bench with dimensions of 1200 × 800 mm was chosen as machine base for the 2D-KCFC test bed shown in Fig. 6a. The base frame made of mild steel, which carries the secondary parts (magnet yokes) of the voice coil motors, is located on this table. The secondary parts can be firmly bolted to the base frame via solid spacers (Fig. 6a) or flexibly connected to the frame via leaf springs (Fig. 6c) or rubber spacers (Fig. 6d). This additional decoupling can be applied in order to reduce the excitation of tilting vibrations, caused by the application of forces in two different *Z*-planes (torque excitation).

The guiding system is based on a cross guide consisting of miniature profile rail guides. Linear scales for position measurement are arranged next to these rails. The cross guide realises the stiffness in *Z*-direction only, while the stiffness in *X*- and *Y*-direction is generated by the position control loops. In order to be able to decouple the accuracy relevant guide system from the base frame, it is mounted on a separate guide frame made of mild steel. The guide frame is fixed with compliant connecting elements. By using rubber springs as connecting elements the guide frame can be decoupled from the base frame and thus from force flow in the *X*- and *Y*-direction. This also reduces the transmission of vibrations induced at the magnets. For reasons of clarity, the drag chains, switch cabinet and enclosure are not depicted in Fig. 6.

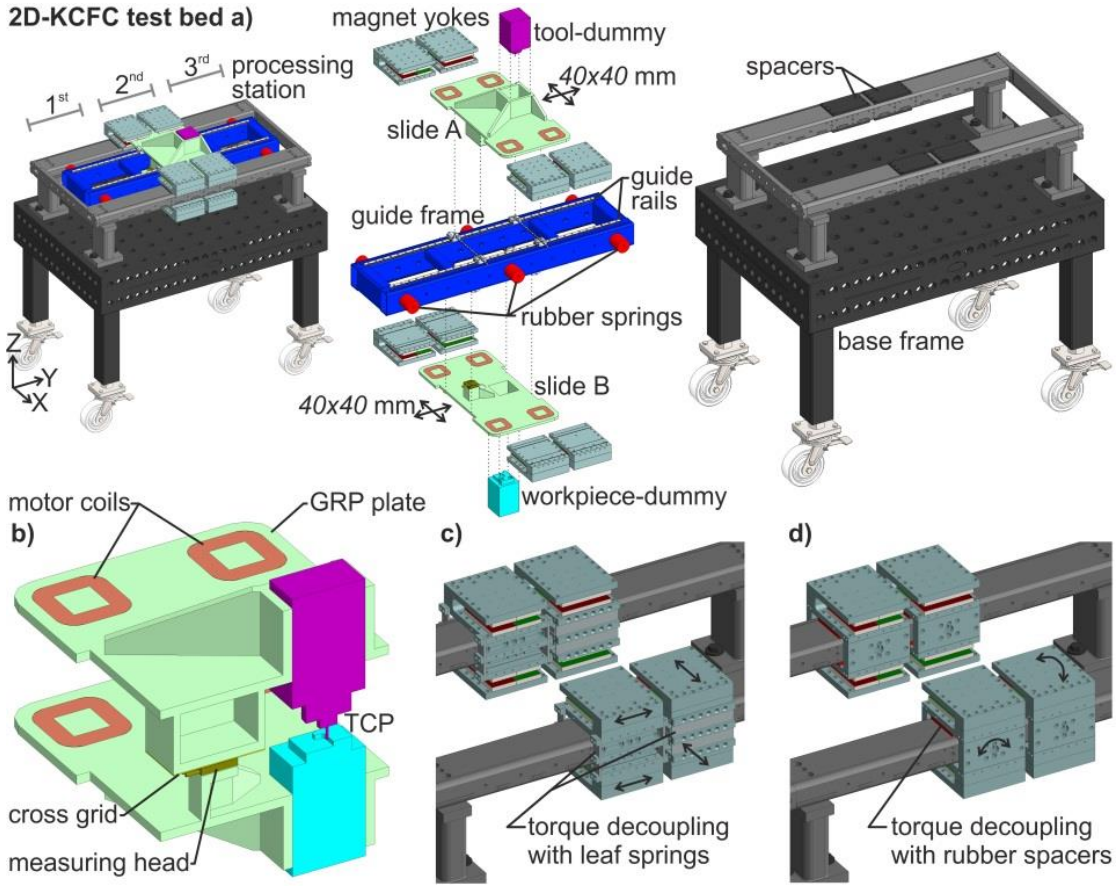

Fig. 6. 2D-KCFC test bed: a) overview of the components, b) detail of the slides, c), d) mechanical decoupling

The frame structure is designed to provide a total of three processing stations (suggested in Fig. 6a as 1st to 3rd processing station). The KCFC processing station is situated in the middle and can be approached by two lower slide plates alternately. The two outer stations are initially used for manual loading and unloading of workpieces or tools and will later be supplemented by simple machining stations. The slide plates form the core component of the motion system. They have to be lightweight and rigid as well as electrically non-conductive. An electrical conductor such as aluminium or even carbon fibre reinforces plastic (CFRP) would cause an undesirable decelerating or damping effect as well as additional

heating as a result of the eddy currents induced during motion within the magnet yokes. Therefore, a glass-fibre reinforced plastic (GRP) of type FR4 was chosen for the construction of the slide plates.

For the lightweight design of the slides, a topology optimisation was carried out. The total mass was minimised with the aim of maximum static stiffness and highest possible natural frequencies. The material properties of FR4 were homogenised for this purpose. The geometry thus obtained was then reproduced as a ribbed slide plate with the FR4 plate thicknesses available on the market, whereby a mass of approximately 4.8 kg was achieved for the slide plate with coils (see Fig. 6b). The Z-axis units are initially assumed to have an equivalent mass of 5 kg. In Fig. 6b the arrangement of the planar measuring system is shown.

A simulative modal analysis was performed using ANSYS Workbench Software to evaluate the mechanical structure of the 2D-KCFC motion system. Fig. 7a shows the meshed components. The welding bench was elastically supported at its four feet and the stiffness of the supports was adjusted by means of an experimental modal analysis of the table without superstructures. The resulting stiffness of the linear guides in the Z-direction was assumed to be 35 N/µm each.

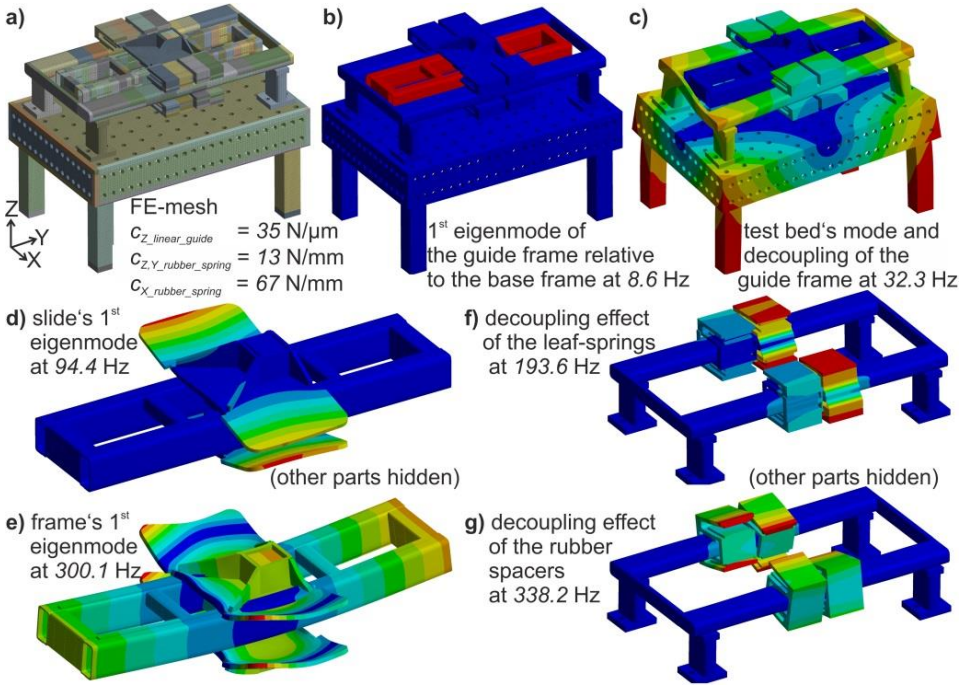

Fig. 7. FE modelling and modal analyses of the KCFC test bed

The parameterisation of the six rubber springs for the mounting of the guide frame in the base frame (see Fig. 6a and Fig. 7a) is based on metal-rubber elements from the supplier Mädler GmbH. The decoupling effect which can be achieved by application of six rubber springs becomes clear in Fig. 7b by means of the first translatory eigenmode (*Y*-direction) of the guide frame mounted in the base frame. This arrangement behaves like a mechanical low-pass filter. Higher-frequency excitations from the base frame or the drive system are attenuated before they are transmitted to the guide frame (see also eigenmode at 32.3 Hz in

Fig. 7c). In addition, by decoupling the secondary parts from the base frame, the structural excitation resulting from torque excitation can be reduced. Fig. 7f shows the relevant eigenmode of the decoupling arrangement with leaf springs (see also Fig. 6c). Fig. 7g depicts the corresponding eigenmode of the decoupling arrangement with rubber spacers (see also Fig. 6d).

With the dimensions selected for the leaf springs (thickness 2 mm) and the shape and material selected for the rubber spacers, the corresponding natural frequencies are relatively high, which leads to the expectation of a low decoupling effect. The final dimensioning of the torque decoupling should be carried out considering reliable, experimentally validated damping values.

Fig. 7d shows the first eigenmode of the slides at approximately 94 Hz. This mode is dominated by the masses of the motor coils. The first eigenmode of the guide frame (see Fig. 7e) is approximately 300 Hz. Overall, the developed machine structure with its modular design offers a wide range of possible configurations for experimental investigation, especially considering the mechanical decoupling of accuracy relevant components.

5. DESIGN OF THE DRIVE SYSTEM

The drive system is essential for the generation of highly dynamic feed motions. In order to enable a compact and rigid design and to adjust the motor force constant and the force rise rate, voice coil motors are developed in-house. These determine the feed dynamics of the motion system via their force constant k_{Mot} and the coil inductance L_{coil} in interaction with the moving mass of the slides m_A and m_B.

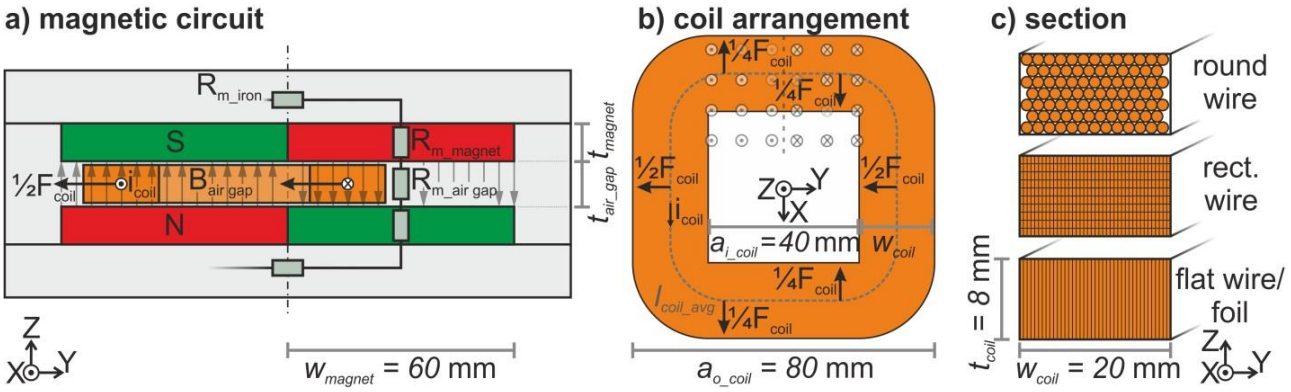

Fig. 8. Magnetic circuit and coil specifications of voice coil drive system

The motors are based on a coil in the magnetic field of permanent magnets (see Fig. 8), whereby the maximum travel distance results from the width of the coil w_{coil} and the magnet width w_{magnet}. In addition, the magnets are longer (in X-direction in Fig. 8a) than the coil dimension $a_{\mathrm{o\_coil}}$, so that the coils can also be moved 40 mm in this direction without leaving the magnetic field. In this arrangement, only two of the four coil sections generate a

feed force ($2 \cdot ½ F_{\text{coil}}$ in Fig. 8b), while the forces acting in the other two coil sections stress the coil on shear ($4 \cdot ¼ F_{\text{coil}}$ in Fig. 8b). The simple design depicted in Fig. 8 was chosen because it promises high feed dynamics with moderate manufacturing effort and, in addition enables the slides to be moved out of the U-shaped secondary parts in *Y*-direction in order to approach the other processing stations (see Fig. 6a).

For the design of the drive system, the magnetic field in the air gap must be known. For this, the magnetic circuit is abstracted according to Fig. 8a with magnetic equivalent resistors $R_{\text{m\_i}}$. The field in the air gap $B_{\text{air\_gap}}$ is determined using Eq. (1) to (3), which have been derived from [16]. The magnetic resistance of the ferromagnetic circle $R_{\text{m\_iron}}$ and the stray field of the magnets are neglected. The most important design parameters are thus the height of the air gap $t_{\text{air\_gap}}$, the magnet thickness t_{magnet} and the remanence flux density $B_{\text{R\_magnet}}$ of the magnet material. Neodymium magnets with a thickness of $t_{\text{magnet}} = 10$ mm in the magnetisation N45 ($B_{\text{R\_magnet}} = 1.35$ T and $\mu_{\text{rel\_magnet}} = 1.05$) are considered. For the air gap, a value of $t_{\text{air\_gap}} = 12$ mm was chosen for design reasons (thickness of the slide plate 10 mm). This results in an air gap field of $B_{\text{air\_gap}} = 0.83$ T, derived from Eq. (3).

$$\phi \cdot R_{\text{m\_magnet}} + \phi \cdot R_{\text{m\_air gap}} = \theta_{\text{eq\_magnet}} = \phi_{\text{R\_magnet}} \cdot \frac{\sum t_{\text{magnet}}}{\mu_0 \cdot \mu_{\text{magnet}} \cdot A_{\text{magnet}}} \tag{1}$$

considering: $R_m = \frac{l}{\mu_0 \cdot \mu_{\text{rel}} \cdot A}$, $A = A_{\text{magnet}} = A_{\text{air\_gap}}$ and $\phi = B \cdot A$ leads to:

$$B \cdot \left(\frac{\sum t_{\text{magnet}}}{\mu_0 \cdot \mu_{\text{rel\_magnet}}} + \frac{t_{\text{air\_gap}}}{\mu_0 \cdot \mu_{\text{rel\_air gap}}} \right) = B_{\text{R\_magnet}} \cdot \frac{\sum t_{\text{magnet}}}{\mu_0 \cdot \mu_{\text{rel\_magnet}}} \tag{2}$$

Considering $\mu_{\text{rel\_air gap}} = 1$ and $\sum t_{\text{magnet}} = 2 \cdot t_{\text{magnet}}$ Eq. (2) leads to the equation of proportion for the magnetic field in the air gap:

$$B = B_{\text{air\_gap}} = \frac{B_{\text{R\_magnet}} \cdot (2 \cdot t_{\text{magnet}} / \mu_{\text{magnet}})}{(2 \cdot t_{\text{magnet}} / \mu_{\text{magnet}} + t_{\text{air\_gap}})} \tag{3}$$

With the air gap field and the effective conductor length ($½ \cdot l_{\text{coil\_avg}} \cdot N_{\text{coil}}$, see Fig. 8b for $l_{\text{coil\_avg}}$) in the magnetic field, the motor force constant k_{Mot} can be calculated according to (4):

$$k_{\text{Mot}} = \frac{1}{2} \cdot l_{\text{coil\_avg}} \cdot N_{\text{coil}} \cdot B_{\text{air\_gap}} \,. \tag{4}$$

Considering Fig. 8c the coil winding can be carried out in three basic winding variants. The winding with round wire has the lowest filling factor. The winding variants with rectangular or flat wire (foil winding) offer a more compact and, e.g. by baking of self bonding wire, mechanically more stable winding. Using Eq. (5) to (9) the winding variants can be compared with regard to the achievable feed dynamics. The voltage U_{PWM} applied to the coil in interaction with the inductance L_{coil} is decisive for the achievable force rise rate and thus the maximum jerk j_{max} according to (8). Considering (9), the frequency of the pulse width modulation f_{PWM} determines the value of the current ripple Δi_{coil}, which is present in the coil when i_{coil} is set to zero, i.e. at 50 % duty cycle of the PWM.

$$L_{\text{coil}} = 8 a_{\text{coil}} \cdot {N_{\text{coil}}}^2 \cdot \left[\left(\ln \frac{2 \cdot {a_{\text{coil}}}^2}{t_{\text{coil}} + w_{\text{coil}}} - \ln 2.414 \cdot a_{\text{coil}} \right) + \left(0.914 + 0.2235 \frac{t_{\text{coil}} + w_{\text{coil}}}{a_{\text{coil}}} \right) \right] \tag{5}$$

from [17] with: a_{coil}, t_{coil}, w_{coil} in cm; L_{coil} in nH; $a_{\mathrm{coil}} = \frac{a_{\mathrm{o\_coil}} + a_{\mathrm{i\_coil}}}{2}$; $w_{\mathrm{coil}} = \frac{a_{\mathrm{o\_coil}} - a_{\mathrm{i\_coil}}}{2}$

$$v_{\max} = \frac{U_{\mathrm{PWM}}}{k_{\mathrm{Mot}}} \tag{6}$$

$$a_{\max} = \frac{k_{\mathrm{Mot}} \cdot i_{\max}}{(m_{\mathrm{slide}} + m_{\mathrm{tool/workpiece}})} \tag{7}$$

$$j_{\max} = \frac{U_{\mathrm{PWM}}}{L_{\mathrm{coil}}} \cdot \frac{k_{\mathrm{Mot}}}{(m_{\mathrm{slide}} + m_{\mathrm{tool/workpiece}})} \tag{8}$$

$$\Delta i_{\mathrm{coil}} = \frac{U_{\mathrm{PWM}}}{2 \cdot L_{\mathrm{coil}} \cdot f_{\mathrm{PWM}}} \tag{9}$$

Table 1 compares the three winding types shown in Fig. 8c with respect to their dynamic potential, assuming almost identical conductor cross-sections.

Table 1. Comparison of different winding types ($v_{\max}$, $a_{\max}$, $j_{\max}$ for a slide $m_{\mathrm{A,B}}$ = 10 kg with two coils; U_{PWM} = 100 V)

Parameter	Round wire	Rect. wire	Flat wire
dimensions with/w.o. insulation in mm	0.684 / 0.60	2·0.2 / 1.94·0.14	8·0.055 / 8·0.035
number of windings and sect. in mm²	354 / 0.282	400 / 0.272	363 / 0.280
L_{coil} in mH and R_{coil} in Ω	9.5 / 4.8	12.2 / 5.6	10.1 / 4.9
force constant k_{MOT} in N/A	32.7 (100 %)	36.9 (113 %)	33.5 (103 %)
max. speed $v_{\max}$ in m/s	3.06 (100 %)	2.71 (89 %)	2.99 (98 %)
max. acceleration $a_{\max}$ in m/s²	65.3 (100 %)	73.8 (113 %)	67.0 (103 %)
max. jerk $j_{\max}$ in m/s³	68435 (100 %)	60367 (89 %)	66473 (97 %)
Δi_{coil} at 16 / 100 kHz PWM in A	0.327 / 0.052	0.256 / 0.041	0.310 / 0.050

It turns out, that the winding with rectangular wire and foil winding enable a higher motor force constant k_{Mot} due to their higher filling factor. However, similar dynamic values are achieved as with the winding with round wire. In summary, all the winding variants listed in Table 1 satisfy the required feed dynamics when the superposition of motion at the TCP is considered ($K_{\mathrm{m}} \approx 1$).

According to the high PWM frequency to be selected and the high feed dynamics, a fast control system shall be realised. For this purpose, servo amplifiers, e.g. those of the Triamec Motion AG, offering 100 kHz PWM frequency as well as a cascade control in which position, speed and current control loops are sampled at 100 kHz [18] should be used.

6. SUMMARY AND OUTLOOK

This paper presents the design approach for high-dynamic planar motion systems based on the principle of Kinematically Coupled Force Compensation (KCFC). Starting from a short introduction considering the fundamental conflict between productivity and workpiece quality, approaches to increase feed dynamics while maintaining motion accuracy including KCFC are presented. Applications similar to the concept of KCFC are introduced and processes with highly dynamic motion requirements are presented exemplarily. Subsequently, the specifications for a 2D-KCFC motion system are defined and three possible drive configurations are developed and compared. It was found that an arrangement with four small drives has the lowest moving mass and also allows a favourable support distance a_{rail} between

the linear guides. This concept was designed in detail and equipped with mechanical decoupling elements for the accuracy relevant guide frame. In addition, two designs for the reduction of torque excitation – an elastic connection of the motor secondary parts via leaf springs or rubber spacers – were developed. With a simulative modal analysis of the entire motion system, the decoupling effect of the elastic suspension of the guide frame and the secondary parts (magnets) was demonstrated, whereby for the rubber spacers there is still a need for optimisation with regard to the lowest possible natural frequency.

For the design of each of the four identical voice coil motors of the slide assemblies, the magnetic circuit was first abstracted and the magnetic flux density in the air gap was obtained. Based on this the motor force constant as well as the characteristic dynamic values of the drives could be determined. Three different winding variants comprising round wire, rectangular wire and foil winding were compared. The winding using rectangular wire and foil winding proved to be superior, especially as they offer a higher mechanical stability than the winding with round wire due to the flat mechanical contact between the conductors. The required feed dynamics can be provided by all three dimensioned windings, taking into account the distribution of motion at a ratio of approx. 1:1. Thus, the 2D-KCFC motion system designed in this paper enables precise motion at highest feed dynamics ($v_{max\_TCP} > 2$ m/s, $a_{max\_TCP} > 100$ m/s², $j_{max\_TCP} > 100000$ m/s³). For further mechatronic system design, a point mass model is currently being implemented in MATLAB/Simulink. As shown in Fig. 9, this model comprises the physical domains of mechanics, electrics and thermal transfer as well as the test bed's control system, enabling the evaluation of the interaction of all components.

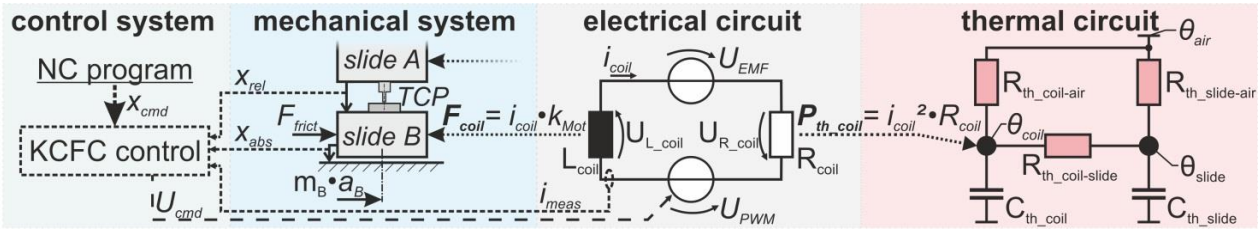

Fig. 9. Scheme of multi-domain simulation model with the physical domains mechanics, electrics and thermal transfer

Beside the implementation of the point mass model, the design of the mechanical components (e.g. by consideration of the anisotropic stiffness of the materials of the slide plates) and the voice coil motors (e.g. by FE analysis of the magnetic circuit) will be improved. Finally, the multi-domain point mass model will be extended to a Multibody-Simulation (MBS) model comprising elastic bodies. This will enable simulation-based analyses and extrapolation of data obtained in experiments using the real 2D-KCFC motion system.

ACKNOWLEDGEMENTS

This research was funded by the German Research Foundation (DFG) within the project „Development and analysis of principles for Kinematically Coupled Force-Compensation for machine tools" (IH124/8-2), which is gratefully acknowledged. Additional thanks go to Clemens Kumpe who supported us with topology optimisation of the slide plates.

REFERENCES

[1] PEUKERT C., MERX M., MÜLLER J., IHLENFELDT S., 2017, *Flexible coupling of drive and guide elements for parallel-driven feed axes to increase dynamics and accuracy of motion*, Journal of Machine Engineering, 17/2, 77–89.

[2] KOREN Y., LO C.C., 1992, *Advanced controllers for feed drives*, CIRP Annals, 41/2, 689–698, https://doi.org10.1016/S0007-8506(07)63255-7.

[3] HIPP K., UHRIG M., HELLMICH A., SCHLEGEL H., NEUGEBAUER R., 2016, *Combination of criteria for controller parameterization in the time and frequency domain by simulation-based optimisation*, Journal of Machine Engineering, 16/4, 70–81.

[4] N.N., 2013, *Mehr Performance mit Parallelkinematik*, Mikroproduktion, 4, 66–68.

[5] TÜLLMANN U., 2009, *Direktantriebe im Einsatz an hochdynamischen Werkzeugmaschinen*, Tagungsband zum 14. Dresdner Werkzeugmaschinen-Fachseminar: Lineardirektantriebe in Werkzeugmaschinen, 243–264.

[6] GROßMANN K., MÜLLER J., MERX M., PEUKERT C., 2014, *Reduktion antriebsverursachter Schwingungen*, Antriebstechnik, 53/4, 35–42.

[7] German patent specification DE102012101979B4.

[8] IHLENFELDT S., MÜLLER J., PEUKERT C., MERX M., 2018, *Kinematically coupled force compensation - experimental results for the 1D-implementation*, 14th Internat. Conference on High Speed Machining, Donostia/San Sebastian, 17–18.04.2018.

[9] ZENTNER J., 2005, *Zur optimalen Gestaltung von Parallelkinematikmaschinen mit Planarantrieben*, Doct. Thesis, TU Ilmenau.

[10] VERL A., HOFFMEISTER H.-W., WURST K.-H., HEINZE T., GERDES A., KALTHOUM M., 2012, *Kleine Werkzeugmaschinen für kleine Werkstücke,* wt Werkstattstechnik online, 102/11/12, 744–749.

[11] European patent specification EP0523042B1.

[12] AMANN E., 2012, *Modeling and motion control of a pick and place machine with air bearings*, Master of Science Thesis, KTH Industrial Engineering and Management, Stockholm.

[13] HARMAN G., 2010, *Wire bonding in microelectronics*, 3rd Edition, McGraw Hill, New York.

[14] CHEN X., BAI Y., YANG Z., GAO J., CHEN G., 2015, *A precision-positioning method for a high-acceleration low-load mechanism based on optimal spatial and temporal distribution of inertial energy*, Engineering, 1/3, 391–398, https://doi.org/10.15302/J-ENG-2015063.

[15] HIRAMOTO K., HANSEL A., DING S., YAMAZAKI H., 2005, *A study on the drive at the Center of Gravity (DCG) feed principle and its application for development of high performance machine tool systems*, CIRP Annals – Manufacturing Technology, 54/1, 333–336, https://doi.org/10.1016/S0007-8506(07)60116-4.

[16] MARINESCU M., 2012, *Elektrische und magnetische Felder*, 3rd Edition, Springer, Heidelberg, Dordrecht, London, New York.

[17] HERTWIG H., 1954, *Induktivitäten*, Verlag für Radio-Foto-Kinotechnik, Berlin.

[18] https://www.triamec.com/de/servo-drives.html.